RESEARCH ARTICLE

Brain Pathology

Neuropathological and cerebrospinal fluid correlates of choroid plexus inflammation in progressive multiple sclerosis

R. Magliozzi[1,2] | S. Hametner[3,4] | M. Mastantuono[1] | A. Mensi[1,5] |
M. Karimian[1] | L. Griffiths[6] | L. M. Watkins[6] | A. Poli[1] | G. M. Berti[1] |
E. Barusolo[1] | B. Bellini[1] | S. Rossi[7] | D. Gveric[2] | J. A. Stratton[8] |
K. Akassoglou[9,10,11] | S. Magon[12] | R. Nicholas[2] | R. Reynolds[2] |
O. W. Howell[6] | S. Monaco[1]

[1]Neurology Section of Department of Neuroscience, Biomedicine and Movement, University of Verona, Verona, Italy

[2]Department of Brain Sciences, Faculty of Medicine, Imperial College London, London, UK

[3]Division of Neuropathology and Neurochemistry, Department of Neurology, Medical University of Vienna, Vienna, Austria

[4]Comprehensive Center for Clinical Neurosciences and Mental Health, Medical University of Vienna, Vienna, Austria

[5]Department of Computer Science, University of Verona, Verona, Italy

[6]Institute of Life Sciences, Swansea University, Swansea, UK

[7]Department of Oncology and Molecular Medicine, Istituto Superiore di Sanità, Rome, Italy

[8]Department of Neurology and Neurosurgery, McGill University, Montreal, Canada

[9]Gladstone Institute of Neurological Disease, San Francisco, California, USA

[10]Center for Neurovascular Brain Immunology at Gladstone and UCSF, San Francisco, USA

[11]Weill Institute of Neurosciences and Department of Neurology, University of California, San Francisco, San Francisco, California, USA

[12]Roche Pharma Research and Early Development, Roche Innovation Center Basel, F. Hoffmann-La Roche Ltd., Basel, Switzerland

Correspondence
R. Magliozzi, Neurology Section of Department of Neurological and Movement Sciences, University of Verona, Verona, Italy.
Email: roberta.magliozzi@univr.it

Abstract

Among the intrathecal inflammatory niches where compartmentalized inflammation persists and plays a pivotal role in progressive multiple sclerosis (MS), choroid plexus (CP) has recently received renewed attention. To better characterize the neuropathological/molecular correlates of CP in progressive MS and its potential link with other brain inflammatory compartments, such as perivascular spaces and leptomeninges, the levels, composition and phenotype of CP immune infiltration in lateral ventricles of the hippocampus were examined in 40 post-mortem pathologically confirmed MS and 10 healthy donors, using immunochemistry/immunofluorescence and in-situ sequencing. Significant inflammation was detected in the CP of 21 out of the 40 MS cases (52%). The degree of CP inflammation was found correlated with: number of CP macrophages (R: 0.878, $p = 1.012 \times 10^{-13}$) and high frequency of innate immune cells expressing the markers MHC-class II, CD163, CD209, CD11c, TREM2 and TSPO; perivascular inflammation (R: 0.509, $p = 7.921 \times 10^{-4}$), and less with meningeal inflammation (R: 0.365, $p = 0.021$); number of active lesions (R: 0.51, p: 3.524×10^{-5}). However, it did not significantly correlate with any

Hametner S., Mensi A., and Mastantuono M. are equally contributed in this study.

Reynolds R., Howell O.W., and Monaco S. share senior authorship.

clinical/demographic characteristics of the examined population. In-situ sequencing analysis of gene expression in the CP of 3 representative MS cases and 3 controls revealed regulation of inflammatory pathways mainly related to 'type 2 immune response', 'defense to infections', 'antigen processing/presentation'. Analysis of 78 inflammatory molecules in paired post-mortem CSF, the levels of fibrinogen (R: 0.640, $p = 8.752 \times 10^{-6}$), PDGF-bb (R: 0.470, $p = 0.002$), CXCL13 (R: 0.428, $p = 0.006$) and IL15 (R: 0.327, $p = 0.040$) were correlated with extent of CP inflammation. Elevated fibrinogen and complement deposition were found in CP and in underlying subependymal periventricular areas, according to "surface-in" gradient associated with concomitant prominent microglia activation. CP inflammation, predominantly characterized by innate immunity, represents another key determinant of intrathecal, compartmentalised inflammation persisting in progressive MS, which may be possibly activated by fibrinogen and influence periventricular pathology, even without substantial association with clinical features.

1 | INTRODUCTION

A key feature of MS is the persistent inflammatory activity in the CNS throughout the whole disease course. Disruption of the blood–brain barrier (BBB) and perivascular lymphocyte infiltration are associated with focal demyelination in early disease. In progressive forms, disease severity is related to a prevailing CNS-specific innate immune response, with persistent cellular infiltrates of the leptomeninges and perivascular spaces, and consequent accumulating tissue damage. It has been shown that T and B cells, and monocyte-macrophages survive and persist in the CNS, becoming trapped or compartmentalized in perivascular Virchow-Robin spaces, the leptomeninges, and possibly the CP [1–4].

The cerebrospinal fluid (CSF) filled spaces may represent a CNS compartment contributing to and sustaining an intrathecal inflammatory milieu, and an underlying gradient of tissue injury, impacting on disease activity and progression [3, 5]. The finding of MS-specific CP increased volume in MS patients compared to healthy controls and NMOSD and patients with migraine [6–9], clinically isolated syndrome (CIS) [10] and in pediatric MS [11] further underlines the potential MS-specific involvement of the CP in the disease. In particular, recent studies demonstrated that the CP volume enlargement may contribute to cognitive impairment and fatigue, increase of paramagnetic rim lesions and chronic lesion expansion [9, 10, 12, 13]. However, it remains unclear whether the progressive CP enlargement in patients may reflect any relevant inflammatory events and whether current disease modifying therapies enter these compartments at sufficient concentrations to affect the related inflammatory processes and whether their targets are indeed present.

Experimental and clinical evidence suggests that intrathecally compartmentalized inflammation may play a crucial role in the severity and rate of MS progression [3, 14, 15]. Strikingly, in a substantial proportion of cases, cortical and thalamic atrophy and damage appear to follow a "surface-in" gradient, more pronounced in the areas near to CSF-filled spaces as opposed to more distal areas. This gradient of injury suggests that diffusion of inflammatory/toxic factors from the CSF can drive superficial cell/molecular alterations and tissue atrophy [16–18]. Recent combined pathology-molecular studies demonstrated the "surface-in" damage was linked to intrathecal inflammation, specifically to CSF-associated meningeal inflammation, extensive cortical pathology, and a more rapid and severe MS course [15]. The same intrathecal signature of CSF-inflammation was present in clinical cases sampled at early diagnosis and characterized by a higher burden of cortical pathology. The CP represents one of the main routes of traffic of inflammatory cells and factors into the CNS, where it may strongly contribute to the burden of subependymal/periventricular tissue pathology in MS. Whether CP alterations play a crucial role in MS in intrathecal inflammation and surface-in pathology has yet to be investigated.

We aimed to test whether CP inflammation may represent one of key components of MS progression. Therefore, we asked the question whether CP inflammation reflects a state of elevated intrathecal inflammation and if CP inflammation associates with an altered CSF immune profile and underlying tissue injury.

2 | MATERIALS AND METHODS

2.1 | Post-mortem tissue sampling

The extent and distribution of inflammatory infiltrates in the CP, meninges and perivascular infiltrates were

examined in formalin-fixed paraffin-embedded (FFPE) tissue blocks containing the hippocampus from post-mortem brains of cases with pathologically confirmed MS (40) and healthy controls (10) using immunohistochemistry/ immunofluorescence. Tissue blocks have been selected according to the presence of well-preserved meningeal and choroid plexus structures. All the MS and control cases were obtained from the UK Multiple Sclerosis Society Tissue Bank (UKMSTB) at Imperial College under appropriate ethical approval (08/MRE09/31). The diagnosis of MS was neuropathologically confirmed according to the International Classification of Diseases of the Nervous System criteria (www.ICDNS.org). Clinical-demographics (gender, age at onset, age at death, disease duration, time to progression, time from progression to wheelchair, disease activity) and neuropathological variables (degree of CP inflammation, number of meningeal follicles, degree of perivascular inflammation, degree of lesion activity) were extensively analyzed for each case (Table 1). In addition, matched tissue blocks from 10 non-neurological controls (mean age: 62.6 ± 17.2 years, 4 male and 6 female) were also examined. The demographic, clinical and neuropathological details of the examined MS and control cases used in this study are summarized in Table 1.

2.2 | Immunohistochemistry and image acquisition

One FFPE tissue block (2×2 cm^2) containing the hippocampus was studied from each brain. From 5 out of the 40 MS cases, whole coronal bi-hemispheric coronal slices captured at the level of the anterior hippocampus, as well as one section approximately 2 cm anterior and 2 cm posterior to this section were included, in order to help visualize the association between CP inflammation and demyelination. Serial FFPE sections (7 μm) were dewaxed and rehydrated in phosphate buffered saline (PBS). Immunohistochemical and immunofluorescence detection of antibodies to MOG, PLP, MHC class II, CD3, CD4, CD8, CD20, CD68, CD163, TMEM 119, DC-Sign, TREM2, TSPO, IL15, CD62L, RASGRP2, fibrinogen and complement components (Table S1) was performed according to previously optimized protocols [17, 19]. Negative controls were included in each experiment and all sections from all cases were stained together in the same experimental run. All sections for immunohistochemistry were counterstained with haematoxylin, sealed with Entellan rapid mounting medium, and viewed with a ZEISS Axioscope microscope (ZEISS International, Germany). Images were captured with a Axiocam 208 Color camera (ZEISS) or with Leica-Aperio microscope scanner. All sections used for immunofluorescence were counterstained with DAPI and viewed with a Leica THUNDER Imager Tissue microscope (Leica Microsystem, Germany).

2.3 | Neuropathology analysis

2.3.1 | Demyelinating activity

The presence, extent and state of the demyelinated lesions both in white matter (WM) and in grey matter (GM) of MS cases were analyzed by combining immunohistochemical detection of myelin oligodendrocyte glycoprotein (MOG) and major histocompatibility complex (MHC) class II with Luxol Fast blue (LFB) staining on serial sections, as previously described [20, 21]. Digital pathology image analysis using QuPath software [22] was used to trace and measure the entire WM and GM fraction for each MOG immunostained section. Then the areas of individual WM and GM lesions were measured to obtain the percentage of demyelinated WM and GM rispect to the total GM or WM.

Inflammatory activity of demyelinating lesions (early active, active, chronic active and chronic inactive) was evaluated based on cellularity, presence of foamy macrophages and perivascular infiltrates, according to previous classification procedures [23–25].

2.3.2 | Immune cell infiltration

In order to obtain a detailed quantitative and qualitative assessment the degree of perivascular lymphocytic and monocytic-macrophage inflammation in the meninges, perivascular spaces, CP of the selected hippocampus block, we used a semi-quantitative scoring previously optimized in our laboratories [14, 17, 26, 27] by counting the number of CD3+, CD20+, and CD68+ cells, regardless the myelin status. Meningeal infiltrates were analyzed along the cortical GM portion of the hippocampus; the perivascular infiltrates have been examined in the white matter portion; finally, the CP infiltrates were examined in the lateral ventricle. In the CP analysis we focus our attention on epithelium and stromal compartments, avoiding intravascular immune cell count as previously demonstrated [28] In particular, we used a modified scoring system: Score 0 corresponds to absent/scarce (0–5 cells), 1 corresponded to moderate (6–25 cells), 2 corresponded to high (26–50 cells), 3 (>51 cells) corresponded to extensive inflammatory infiltrate (Figure 1). Semi-quantitative scoring was performed on three images (contiguous but not overlapping in order to include the complete available CP area) for each MS and Control case acquired at 20× objective in the region of interest (RoI) making sure that the same surface (tissue area = 17,412,885 μm^2) was analyzed in each RoI and taking into account the variable surface areas of the CP in the different sections.

T A B L E 1 Demographic, clinical and neuropathological features of the examined MS and control cases.

MS case	Gender	Age at onset	Time to progression	Time from progression to wc (EDSS7)	Disease duration	Age at death	Disease activity	Degree of CP inflammation	CD3+ cells	CD20+ cells	MHCII+ cells
MS104	M	42	5	0	12	54	0	0	1.33 ± 0.53	1	4
MS230[a]	F	22	13	1	31	53	1	**2**	7.44 ± 1.82	5	11
MS277	F	18	21	6	43	71	0	0	3.22 ± 0.33	1	5
MS296	M	19	27	2	52	71	0	1	4.34 ± 0.89	2	4
MS301	F	43	6	6	27	70	0	0	2.33 ± 0.55	1	4
MS304	M	29	9	4	23	52	1	1	3.53 ± 0.66	2	5
MS311	F	29	4	1	22	51	1	0	2,45 ± 0.23	1	3
MS318	F	25	22	4	44	69	0	1	3.66 ± 0.57	1	6
MS325[a]	M	48	0	1	9	57	1	**2**	13.33 ± 1.52	3	15
MS326	M	29	8	13	42	71	1	0	2.66 ± 0.57	1	3
MS330	F	14	16	3	45	59	1	1	7.33 ± 1.56	3	12
MS347	M	22	26	8	30	52	1	0	2.44 ± 0.55	1	3
MS376	F	38	2	4	20	58	0	0	3.36 ± 0.33	0	4
MS402	M	26	11	2	26	52	0	1	4.66 ± 0.88	2	7
MS407	F	25	9	1	21	46	1	1	3.22 ± 0.44	3	8
MS408	M	29	8	2	20	49	1	1	4.21 ± 0.55	1	6
MS418	M	18	23	4	42	60	1	1	5.63 ± 1.55	2	7
MS423	F	24	9	3	32	56	1	1	6.33 ± 1.44	2	9
MS424	F	29	6	2	10	39	1	0	2.33 ± 0.52	1	3
MS439	F	26	23	7	32	58	0	0	3.42 ± 0.73	1	4
MS473	F	27	NA	8	19	46	1	1	4 ± 1	2	8
MS486	M	NA	NA	NA	NA	64	1	0	3.34 ± 0.66	1	5
MS491	F	38	0	0	28	66	0	0	1.33 ± 0.57	1	3
MS497	F	30	18	0	31	61	1	0	2.66 ± 0.55	0	3.33 ± 0.57
MS500	M	22	NA	8	33	55	1	0	1.33 ± 0.57	1.33± 0.57	3.66 ± 0.33
MS510	F	16	7	0	27	43	1	1	6.54 ± 1.75	2.66± 0.55	9.45 ± 1.25
MS512	F	16	29	NA	47	63	1	0	2.55 ± 0.32	1.33± 0.52	4.66 ± 1.52
MS513	M	33	8	NA	13	46	1	1	5.82 ± 1.24	2± 2.33	8.66 ± 1.26
MS514	F	18	34	4	56	74	1	1	4.32 ± 1.12	1.33± 0.57	9.55 ± 1.52
MS517	F	25	NA	8	28	53	1	0	1.22 ± 0.33	0	3.33 ± 0.57
MS520	M	32	36	0	40	72	1	0	1.33 ± 0.57	0	2.66 ± 0.33
MS527	M	21	10	2	29	50	1	1	4.28 ± 1.25	1.77± 0.33	7.51 ± 1.55
MS533	M	25	NA	0	32	57	1	1	5.33 ± 1.55	1.33± 0.57	9.66 ± 2.57
MS538	M	NA	NA	NA	NA	50	0	0	1.44 ± 0.57	0	3.66 ± 0.88
MS540	F	29	NA	4	29	58	1	0	1.33 ± 0.44	0	2.33 ± 1.53
MS542	F	39	NA	8	27	66	1	1	2.66 ± 0.51	1.66± 0.18	8.33 ± 1.52
MS545	M	22	NA	11	32	54	1	**2**	6.25 ± 1.35	2.66± 1.52	9.66 ± 1.15
MS555	F	36	6	6	22	58	1	0	2.66 ± 0.57	0	3.33 ± 0.25
MS561	F	NA	NA	NA	NA	55	1	0	1.22 ± 0.57	0	3.66 ± 0.57
MS586[a]	F	37	3	NA	20	57	1	**2**	8.55 ± 1.55	3.33± 0.57	9.55 ± 1.45
Healthy donor											
C1[a]	F	NA	NA	NA	NA	66	NA	0	0	0	2
C2	F					85		0	0	0	0
C3	M					93		0	0	0	1
C4	F					35		0	1	0	0
C5[a]	M					60		0	0	0	1

T A B L E 1 (Continued)

MS case	Gender	Age at onset	Time to progression	Time from progression to wc (EDSS7)	Disease duration	Age at death	Disease activity	Degree of CP inflammation	CD3+ cells	CD20+ cells	MHCII+ cells
C6	M					75		0	0	0	0
C7	M					88		0	0	0	1
C8	M					68		0	0	0	2
C9	M					77		0	0	1	0
C10[a]	M					32		0	0	0	1

Abbreviation: NA, non-applicable data for healthy donors.
[a]indicate MS and control cases used for ISS Cartana analysis.

2.3.3 | Semi-quantitative analysis of fibrinogen immunoreactivity

Semi-quantitative analysis of the presence and frequency of cells with fibrinogen immunoreactivity was carried out in the hippocampus of 10 out of the 40 examined MS cases, in both active sub-pial cortical lesions (adjacent to infiltrated meninges) and sub-ependymal lesions (adjacent to infiltrated CP). Different antibodies specific for fibrinogen were tested (Table S1), however, after pre-immune serum adsorption or omission of the primary antibody, the one showing less tissue non-specific immunoreactivity was used in the semi-quantitative analysis (asterisk in Table S1). Four consecutive fields (20× objective to allow the specific identification of fibrinogen cell deposition) were examined, moving from the CSF ependymal interface towards subependymal tissue and from the pial district towards inner cortical layers in the hippocampus, according to the "surface-in" distance from the CSF following procedures previously optimized [17, 29]. In addition, double immunofluorescence was performed to assess the localization of fibrinogen in various cell types, such as neurons (MAP2+), microglia/macrophages (MHC-class II+), and astrocytes (GFAP+). The proportion of each cell type with fibrinogen immunoreactivity was then calculated.

2.4 | In-situ sequencing analysis (Cartana)

By using hybridization-in situ sequencing (Hyb-ISS) technology, the expression of 157 targeted inflammatory genes available for the Cartana system (Table S2) was assessed in the choroid plexus of hippocampus FFPE-tissue blocks from three MS (indicated with asterisk in Table 1) and three age matched healthy donors selected from the neuropathological study [30, 31]. The established Hyb-ISS method based on barcoded padlock probes (PLPs) and amplification through rolling circle amplification (RCA) has shown robust detection of RNA. The unique feature of the ISS method was the probe amplification and the integrated barcoding system that can be decoded across sequential rounds of probing, imaging, and stripping [32]. This technique enables the spatial analysis of a custom immune-related panel of 157 genes at their original location in morphologically preserved tissue sections. The MS and control cases were selected according to the presence of intact choroid plexus structures and the good RNA quality (assessed by in-situ sequencing analysis of reference genes RPLP0 detected in all the examined brain samples) [31]. The protocol was performed according to previously optimized procedures [30].

According to the manufacture procedure, one FFPE section (7 μm thick) from each sample (1–13 and 1–20 mm DIA mm × 7 μm) was prepared for Hyb-ISS being de-waxed, rehydrated, fixed and permeabilized. The following steps includes the library preparation by the PLP's hybridization and ligation: hybridization between gene specific chimeric padlock probes and the targeted RNAs (with an enzymatic reaction that requires a 2 h incubation at 37°C) with an overnight incubation at 37°C; the rolling circle amplification where ligated probes were locally amplified resulting in ISS spots that contain multiple copies of the barcodes, this reaction required an overnight incubation at 30°C. Autofluorescence quenching and fluorescent labeling required that the brain sections were treated with TrueBlack Lipofuscin Autofluorescence Quencher (TLAQ) (Biotium) according to manufactures instructions, for 30 s and immediately washed with PBS. All ISS spots were visualized using an anchor fluorescent label with a 30 min incubation at RT. Using the Nikon Ti2-E microscope with ×20 objective the visualization of the nuclei staining and the anchor were detected to check the image quality. In a pre-scan, the tissue area on the microscope glass slide was defined, the camera exposure optimized, and other settings adjusted using Nikon's NIS-Elements software. The sequencing cycles included Bridge probe hybridization: Bridge-probes were hybridized at RT for 1 h in hybridization buffer; readout detection probe hybridization in hybridization buffer for 2 h at RT. The stripping of the signal from the labeling mix (LM) from the previous sequencing cycles was then performed followed by autofluorescence quenching to reduce the autofluorescent background and slides mounting and reading for the

imaging acquisition. Each cycle was repeated 6 times to generate the barcode sequence, them to decode the barcodes of the 157 targeted genes, 6 ISS cycles were required. The identities of all RNA spots, of each ISS cycle of the brain tissue section, was spatially mapped using the Nikon Ti2-E microscope with ×20 objective and sCMOS camera. Thereafter, automated image acquisition, consisting of a variable number of fields of view (20% overlap between individual fields) and 11 z-planes (0.8 μm steps), was performed for five fluorescence channels: blue, to visualize the DAPI and recognize the cell nuclei and other four channels: Alexa Fluor 488, Cy3, Cy5, and Alexa Fluor 750, where ISS spots can be visualized. After image acquisition, the NIS-Elements software, with optimized custom settings for these samples, performed maximum intensity projections, large image stitching and image export by generating and sequencing, directly inside the examined sections, clonally amplified barcode sequences that are introduced by ligation of gene specific probes [30].

2.5 | Post-mortem CSF protein analysis

The levels of 88 inflammatory mediators were determined in the paired CSF samples obtained at time of death from the examined MS and control cases, using custom immune-assay multiplex Luminex technology (Bio-Plex X200 System equipped with a magnetic workstation, BioRad, Hercules, CA, USA), following the procedures previously optimized [15, 17]. For molecules not included in commercially available Luminex assays ELISA immune assays were performed according to procedures previously optimized and published: CSF protein levels of neurofilament light-chain proteins were measured using the ELISA assay #MBS264177 (MyBioSource San Diego, CA, USA) [17]; levels of fibrinogen total antigen using the ELISA assay #MBS135523 (MyBioSource) [15]; levels of parvalbumin (PVALB), a specific marker of cortical GABA-ergic interneurons, with ELISA assay #MBS2022353 (MyBioSource) [17]. All CSF samples were run in duplicate in the same experiment and without knowing group condition. The complete list of the CSF levels (pg/mL) of each molecule analyzed is provided in Table S3.

2.6 | Descriptive analysis and statistical modelling

Descriptive statistics are expressed as mean ± SE or median (IQR) where noted and comparisons were made using non-parametric Mann–Whitney test, Kruskal–Wallis, Friedman test and post-hoc Nemenyi test. Testing for correlations used the Spearman's test corrected by using Bonferroni adjustment. Survival analysis was carried out using the Cox's proportional hazards regression model. A feature selection technique called Random Forest Recursive Feature Elimination (RF-RFE) was used to retain the set of markers with the highest predictive capability of the absence, that is, degree 0, or presence, that is, degree ≥1, CP inflammation. Binary Support Vector Machines with a linear kernel were used to find a rule to predict CP inflammation. For both the RF-RFE analysis and the Support Vector Machines-based one, a Leave One Out cross-validation protocol was adopted. All analyses were performed using MATLAB (MATLAB and Statistics Toolbox, The MathWorks, Inc., Natick, Massachusetts, United States).

3 | RESULTS

3.1 | Choroid plexus immune cell infiltration

Semiquantitative analysis of the degree of inflammation based on the presence of H&E-stained infiltrates in the CP of progressive MS (Table 1, Figure 1) demonstrated considerable CP inflammation (Score >0) in 21 out of the 40 MS cases (52%), but only 4 exhibited a high degree of inflammation (Score 2). Interestingly, CP inflammation never reached a Score 3, which, in contrast, was observed for meningeal and perivascular infiltrates. In addition, organized cell aggregates, similar to the tertiary lymphoid-like structures previously observed in the meninges of the same MS cases, were never detected in the CP. Only along the "tela choroidea" (Figure 2A–D), the thin double-layered membrane created by the pia mater and ependyma (sometimes also called the choroidal fissure), sporadic, small compact cell aggregates containing a moderate number of CD3+, CD20+, and CD68+ cells were identified, but not in the CP portion.

Cell count analysis (Figure 2E–G, J) was performed comparing healthy donors, MS with CP = 0 and MS with CP >0.

Detailed cell count and Spearman correlation analysis demonstrated that degree of CP inflammation was positively correlated with the number of infiltrating T cells (R: 0.855, p: 2.222×10^{-12}), B cells (R: 0.801, p: 5.440×10^{-10}) and macrophages (R: 0.878, p: 1.012×10^{-13}) (Figure 2E–J). As expected, a significant increase of T-cells (vs. MS CP = 0, p: 1.261×10^{-5}; vs. MS CP >0, p: 8.136×10^{-6}), B-cells (vs. MS CP = 0, p: 0.021; vs. MS CP >0, p: 1.094×10^{-5}), and macrophages (vs. MS CP = 0, p: 1.178×10^{-5}; vs. MS CP >0, p: 1.029×10^{-5}) was identified in MS cases compared to controls (Figure 2J). When the absolute number of type of cells were compared, a predominance of macrophages (mean = 8 ± 2.45) was seen with respect to T cells (mean = 5 ± 2.41) and B cells (mean = 2 ± 1.00), which was further validated via a Friedman test (p: 3.398×10^{-9}) and related pairwise post-hoc Nemenyi tests (vs. T cells,
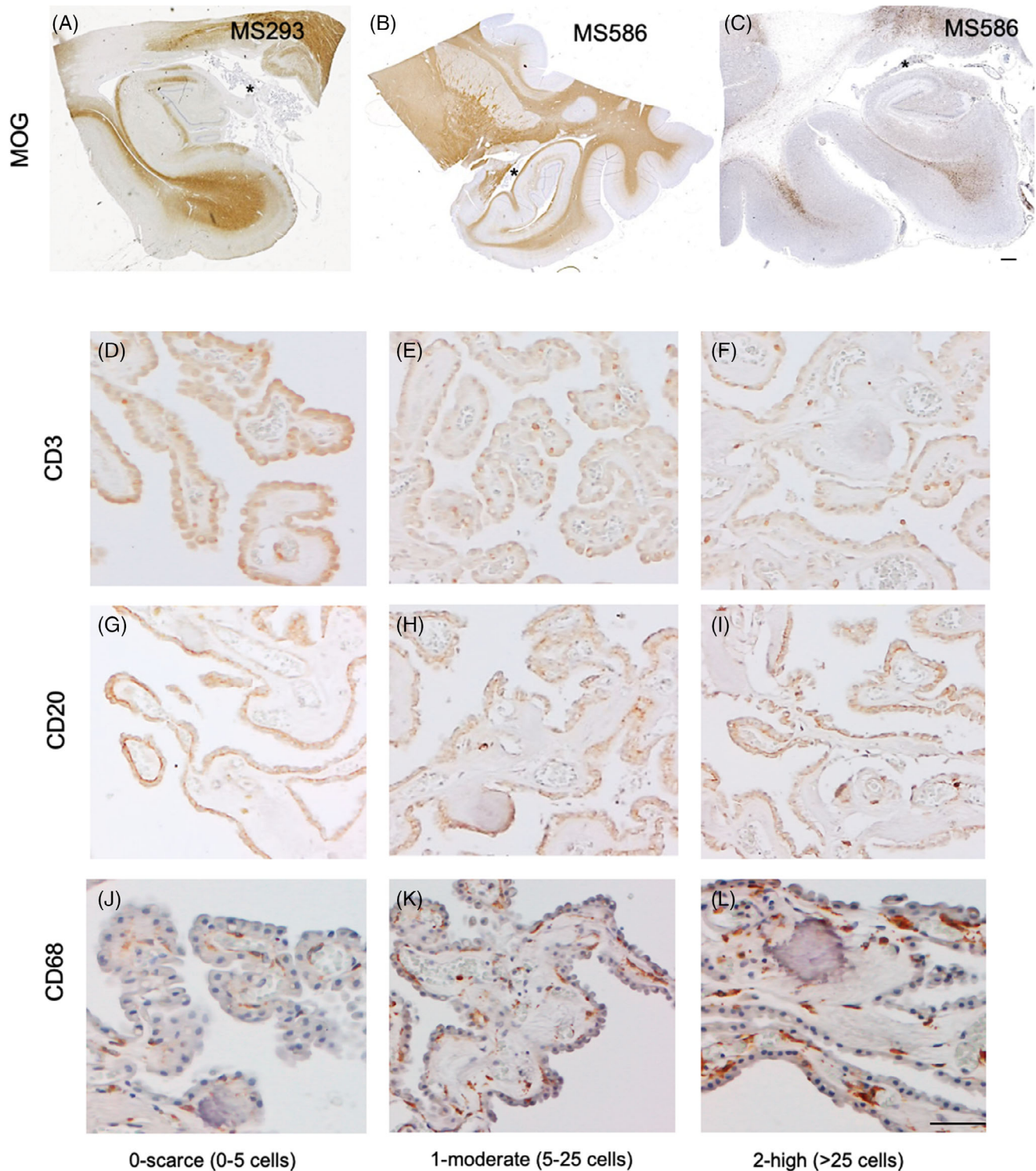
FIGURE 1 Semi-quantitative scoring of CP (indicated by asterisk *) inflammation was performed in the lateral ventricle included in the hippocampus (A–C) of the examined MS cases. By summing the number of CD3+ T cells (D–F), CD20+ B cells (G–I) and CD68+ cells (J–L) for each examined patients the following scores were proposed: Score 0 corresponds to absent/scarce (0–5 cells), 1 corresponds to moderate (6–25 cells), 2 corresponds to high (26–50 cells) inflammatory infiltrate. Scale bars: 1000 μm (A–C), 100 μm (D–L).

p: 0.005; vs. B cells, p: 2.095×10^{-9}; (Figure 2J). Qualitative and semiquantitative comparison between the levels of CD4+ and CD8+ T cells in CP infiltrates suggested preponderance of CD4+ T cells (73%) respect to CD8+ T cells (27%) in the CP of examined MS cases (Figure 2G–I).
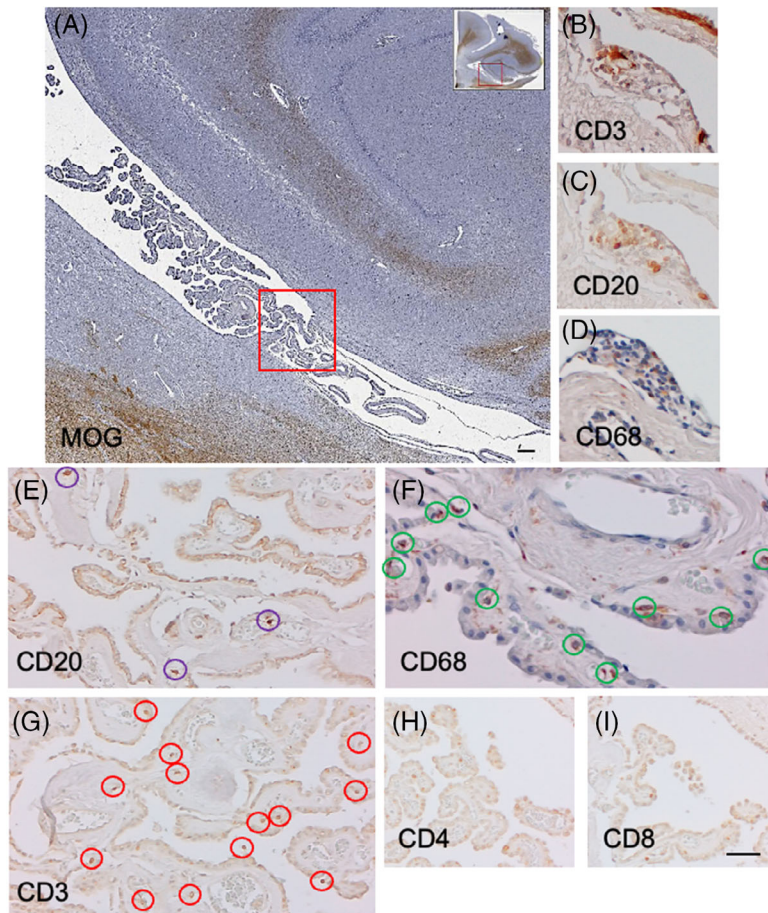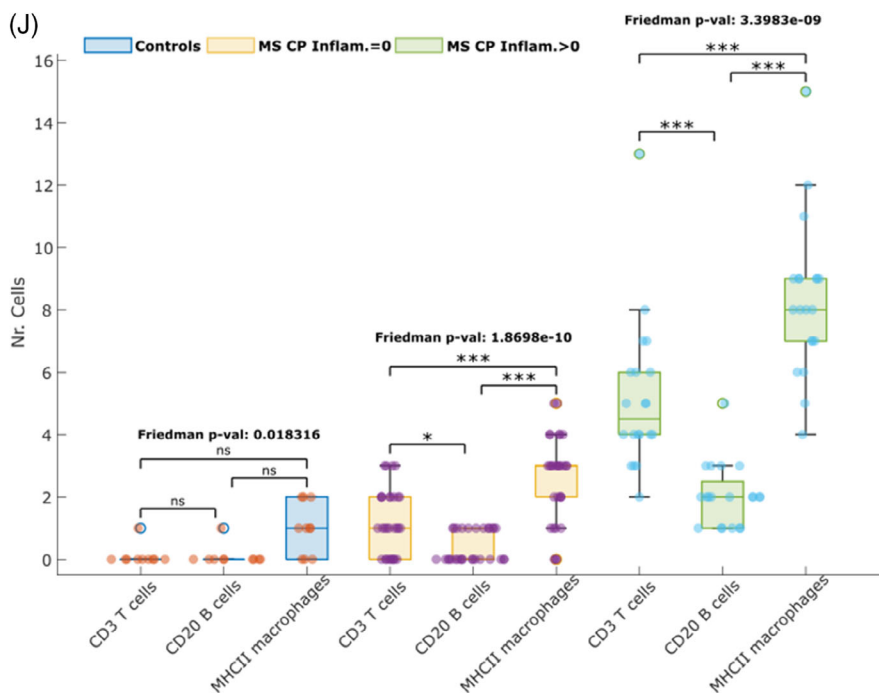
FIGURE 2 Organized lymphocyte aggregates were never detected in the CP. However, in some MS cases, characterized by elevated meningeal inflammation, small compact cell aggregates, CD3+, CD20+, and CD68+ cells, were identified along the "tela coroidea" (square in A and magnifications B–D), while the CP infiltrating cells were mainly found scattered in the stroma. Cell count analysis (E–J) performed comparing 10 healthy donors (light blue), MS with CP = 0 (yellow) and MS with CP >0 (green) demonstrated: significant increase of T-cells (vs. MS CP = 0, p: 1.261×10^{-5}; vs. MS CP >0, p: 8.136×10^{-6}), B-cells (vs. MS CP = 0, p: 0.021; vs. MS CP >0, p: 1.094×10^{-5}), and macrophages (vs. MS CP = 0, p: 1.178×10^{-5}; vs. MS CP >0, p: 1.029×10^{-5}). In addition, the presence of inflammation within the CP was coupled with significant increase of all the type of infiltrating cells (MS CP >0) compared to MS patients characterized by lack of inflammation (MS CP = 0) (T cells p: 3.564×10^{-7}; B cells, p: 2.060×10^{-6}; macrophages, p: 1.006×10^{-7}). Among the CD3+ T cells infiltrating the CP, preponderance of CD4+ T cells was observed (G–I). Scale bars: 500 μm (A), 100 μm (B–I).

3.2 | Preponderance of innate immunity in the choroid plexus of progressive MS brains

Further characterizing the neuropathological features of CP macrophages in progressive MS, frequent MHCII +/CD68+ macrophages, occasionally including intracytoplasmic LFB myelin debris (Figure 3A, inset in A) in the inflamed CP (in MS with CP inflammation>0), mainly in the stromal space between the epithelial and endothelial layers (stromal macrophages). Macrophage CP activity was further characterized by elevated expression of haptoglobin/haemoglobin receptor, CD163 (Figure 3B), of the dendritic cell markers CD209/DCsign (Figure 3C–F) and of the marker of antigen presentation CD11c (Figure 3G,H). Scattered cells expressing the activation myeloid markers TREM2 (Figure 3I,J) were also observed, even if the specific stromal or endothelial localization was not clear. A small amount of scattered CD16+ or CD66b+ granulocytes was also detected, but they were mainly within the CP blood vessels (Figure 3K,L).

3.3 | In-situ sequencing of choroid plexus inflammatory correlates

In-situ gene expression analysis of 157 genes related to inflammation by using in-situ sequencing (ISS) Cartana technique (Figure 4B), revealed significant overexpression (fold change >1.5, $p < 0.05$) of 19 genes (Figure 4C) in the CP of MS compared to control cases, including not only genes validating the neuropathology analysis, such as TSPO and HLA-DRB1, but also several genes that may be involved in recruitment (SELL/CD62L) and activity of immune effector cells, including several inflammatory mediators, such as IL17F, IL15, IL18, IL10, LTB and RASGRP2.

Gene ontology pathway analysis of the 12 genes with >2-fold change in MS CP compared to controls suggested that most of the genes could be associated with biological process regulation of interleukin-2 production, positive regulation of immune effector process, regulation of cytokine production (Figures 4D and S2). From Mammalian Phenotype analysis (MGI) abnormal leukocyte adhesion and physiology, abnormal cellular extravasation, decreased inflammatory response were suggested (Figures 4D and S2). Among the potential pathways suggested by Kyoto Encyclopedia of Genes and Genomes (KEGG) analysis, pathways linked to other chronic inflammatory disease, such as rheumatoid arthritis and inflammatory bowel disease, intestinal immune network for IgA production, Th17 cell differentiation were revealed (Figures 4D and S2). Finally, reactome analysis revealed the prevalence of signaling linked to interleukin-10, interleukin-4 and interleukin-13 (Figures 4D and S2).

By using immunohistochemistry to verify the cell expression of some of these molecules on serial sections used for ISS analysis. We observed scattered cells expressing SELL/CD62L+ (Figure 4E) and RASGRP2 (Figure 4G), while a conspicuous number of cells expressing IL15 (Figure 4F) or TSPO (H,I).

3.4 | Neuropathological and clinical correlates of choroid plexus inflammation

Widespread WM (blue color mask) and GM (cortical and deep GM; red color mask) demyelination was found in MS cases characterized by extensive CP inflammation (Figure 5A), visualized on representative whole coronal sections where available. Lesions were mainly present in periventricular white matter and hippocampus grey and white matter (Figure 5A). The degree of CP inflammation was correlated with the other quantified neuropathological parameters captured across all sampled MS cases. Significant correlations were found between degree of CP inflammation and degree of perivascular inflammation (R: 0.509, p: 7.921×10^{-4}), with meningeal inflammation (R: 0.365, p: 0.021) and with the number of active lesions (R: 0.51, p: 3.524×10^{-5}) identified in the surrounding periventricular areas (Figure 5B). In particular, subependymal periventricular active lesions (Figure 5D) with diffuse activated microglia characterized by elevated expression of MHC-class II, TMEM119, CD163, and iNOS (Figure 5D–H), were detected in the hippocampus of 25 out of the 40 MS cases (62.5%).

The degree of CP inflammation was not correlated with any of the clinical features, such as time from disease onset to progression or from onset to death, of the MS cases (Figure 5I,J). Survival analysis that compared the populations with (red line) and without (blue line) CP inflammation, with respect to the age at death did not found significantly difference (p: 0.391), even if a higher percentage of subjects without CP inflammation were characterized by later age at death (Figure 5J).

3.5 | CSF correlates of choroid plexus inflammation

Among the 78 molecules (8 molecules were removed due to missing values) examined in the CSF of the same MS cases, the degree of CP inflammation correlated with 4 markers: Fibrinogen (R: 0.640, p: 8.752×10^{-6}), PDGF-BB (R: 0.470, p: 0.002), CXCL13 (R: 0.428, p: 0.006) and IL15 (R: 0.327, p: 0.040) (Figure 6A). In particular, CSF fibrinogen levels were significantly higher in MS compared to controls (Figure 6B; p: 0.0001), and were able to discriminate MS with and without CP inflammation ($p = 8.654 \times 10^{-6}$) (Figure 6C).

3.6 | "Surface-in" gradient of fibrinogen deposition in subpial and subependymal lesions

By analyzing fibrinogen immunoreactivity in the hippocampus of the MS and control cases, diffuse fibrinogen deposition
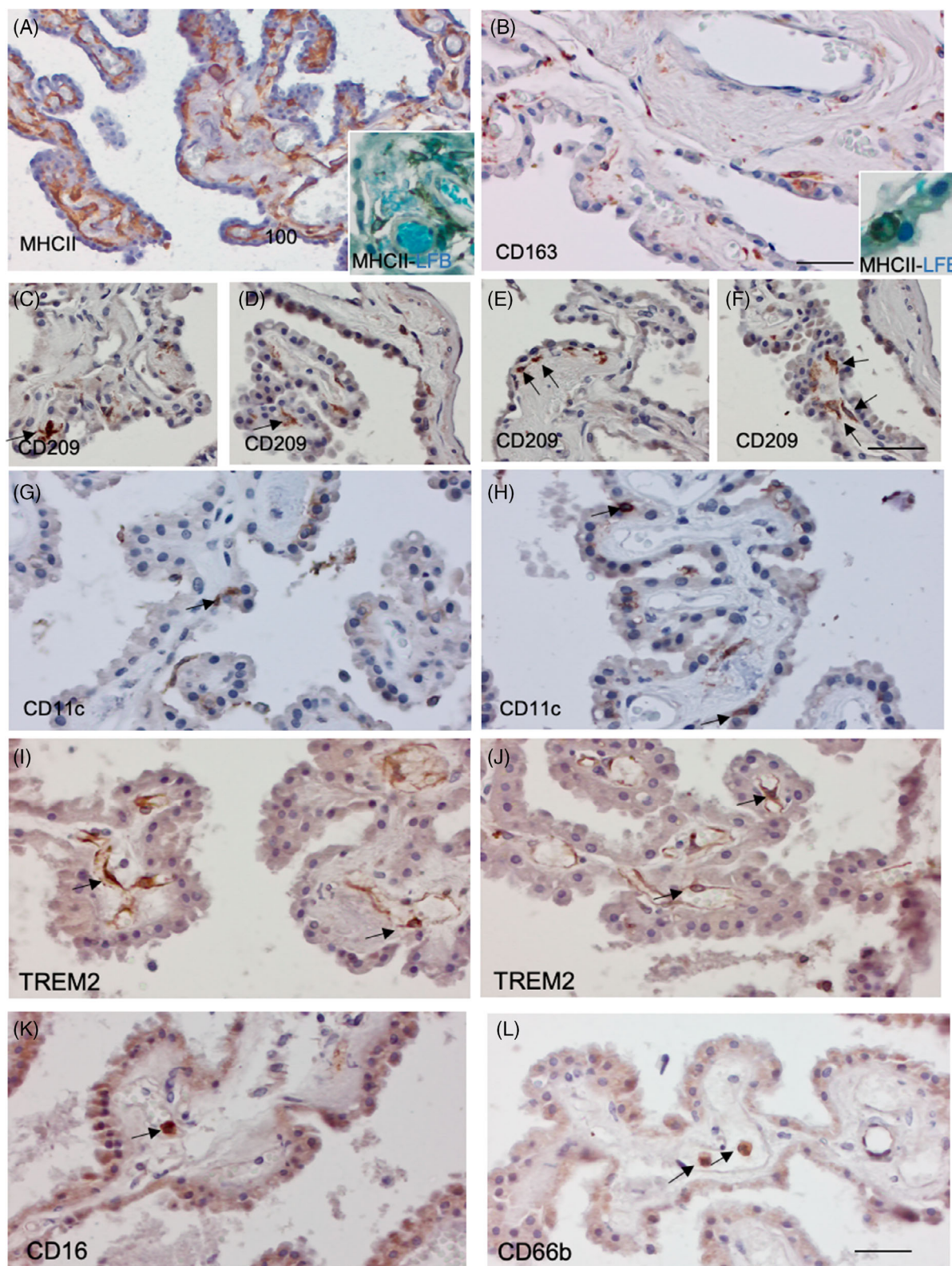
FIGURE 3 Neuropathology characterization of CP innate immune infiltration. Frequent MHCII+ activated macrophages (A), occasionally including intracytoplasmic LFB myelin debris (inset in A and in B), were observed in the inflamed CP (in MS CP >0), mainly in the stromal space between the epithelial and endothelial layers (stromal macrophages). Macrophage CP activity was further characterized by elevated expression of haptoglobin/hemoglobin receptor, CD163 (B), of the dendric cell markers CD209/DCsign (Figure 3C–F, indicated by arrows) and of CD11c, marker of antigen presentation CD11c (G, H, indicated by arrows). Scattered CP infiltrating cells expressing the activation myeloid markers TREM2, sporadically with endothelial morphology and localization (I–J, indicated by arrows) were observed. Only sporadically CD16+ (K, indicated by arrows) or CD66b+ (L, indicated by arrows) granulocytes were detected, predominantly within the CP blood vessels. Scale bars: 100 μm (A–F), 50 μm (G–L).
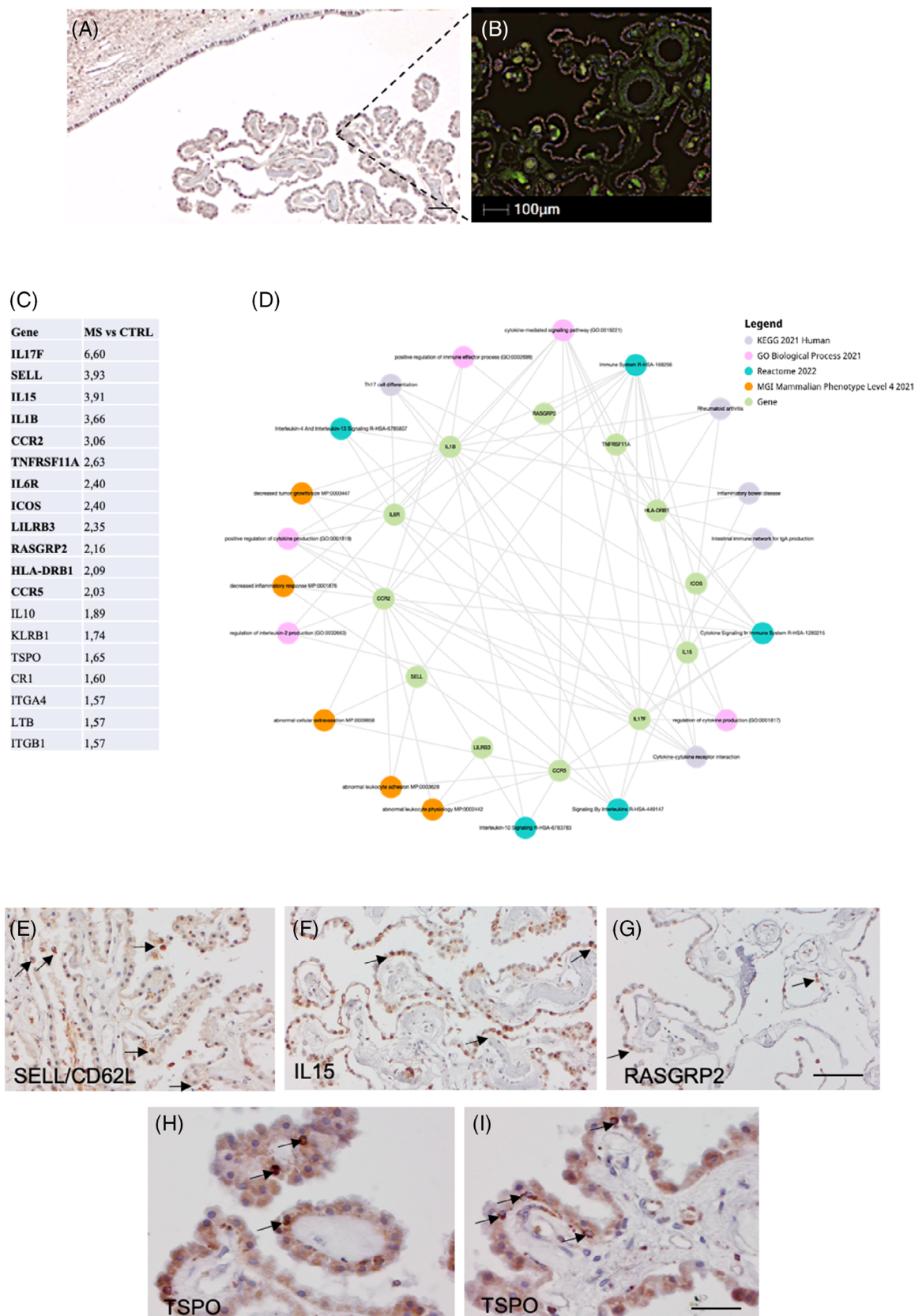
Gene	MS vs CTRL
IL17F	6,60
SELL	3,93
IL15	3,91
IL1B	3,66
CCR2	3,06
TNFRSF11A	2,63
IL6R	2,40
ICOS	2,40
LILRB3	2,35
RASGRP2	2,16
HLA-DRB1	2,09
CCR5	2,03
IL10	1,89
KLRB1	1,74
TSPO	1,65
CR1	1,60
ITGA4	1,57
LTB	1,57
ITGB1	1,57

FIGURE 4 In-situ sequencing (Cartana) of 157 inflammatory genes on the CP of a representative MS case (A, B). List of the 19 genes significant overexpressed (fold change >1.5, $p < 0.05$) in the CP of MS compared to healthy donors (C). Subnetwork analysis of the top 12 genes (fold change >2, $p < 0.05$) (D) extensively explained in Figure S2. Immunohistochemistry validation of some of the significantly deregulated genes found by ISS Cartana analysis, confirmed the presence in the CP on serial brain sections of scattered cells expressing SELL/CD62L+ (E) and RASGRP2 (G), and of frequent cells expressing IL15 (F) or TSPO (H, I). Scale bars: 200 μm (A, B), 100 μm (E–G), 50 μm (G–L).
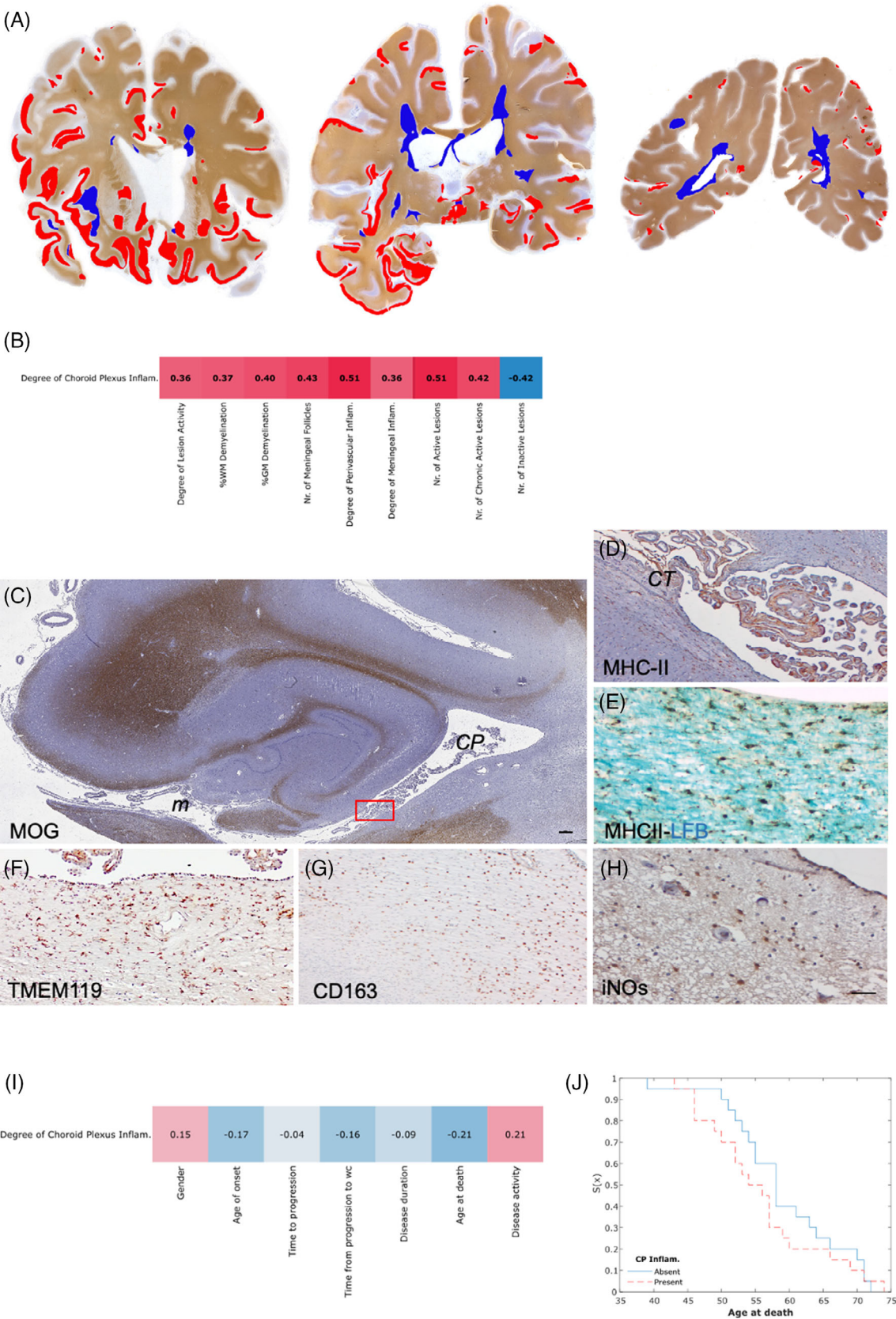
(A)

(B)

Degree of Choroid Plexus Inflam.	0.36	0.37	0.40	0.43	0.51	0.36	0.51	0.42	-0.42

Degree of Lesion Activity · %WM Demyelination · %GM Demyelination · Nr. of Meningeal Follicles · Degree of Perivascular Inflam. · Degree of Meningeal Inflam. · Nr. of Active Lesions · Nr. of Chronic Active Lesions · Nr. of Inactive Lesions

(C) MOG — CP — m

(D) CT — MHC-II

(E) MHCII-LFB

(F) TMEM119

(G) CD163

(H) iNOs

(I)

Degree of Choroid Plexus Inflam.	0.15	-0.17	-0.04	-0.16	-0.09	-0.21	0.21

Gender · Age of onset · Time to progression · Time from progression to wc · Disease duration · Age at death · Disease activity

(J)

S(x) vs Age at death

CP Inflam.: Absent, Present

FIGURE 5 Legend on next page.

was observed in both active sub-pial cortical lesions (Figure 6D–F) and sub-ependymal lesions (Figure 6G,I).

Since fibrinogen distribution was mainly detected in the most superficial layers, close to both the pial or the ependymal surfaces, we aimed to understand if fibrinogen immunostaining would follow a gradient of deposition, greatest near CSF surfaces and reducing towards more distal brain regions (Figure 6O). Neuropathological analyzing in 10 of the MS cases characterized by the presence of at least one of each lesion type revealed fibrinogen immunoreactivity in subpial cortical lesions (Figure 6D–F) or sub-ependymal lesions (Figure 6G–I) in the hippocampus of the examined MS cases, in the area with increased activated microglia density, mainly in cells morphologically resembling microglia, astrocytes or neuronal cells (Figure 6J,K), as validated by double immunofluorescence (Figure 6L–N).

Sub-pial (Figure 6P,Q) and sub-ependymal (Figure 6R,S) gradients of fibrinogen+ cell deposition was detected with an increased density in the areas close to the CSF/brain interface. When the proportion of fibrinogen+ cell types were specifically quantified in the same examined areas by double immunofluorescence cell counting, most of the fibrinogen+ cells were MHC+ microglia/macrophages (59% cortical layer I in subpial lesions, Figure 6Q; 53% field I in subependymal lesions, Figure 6S), in particular in the most external areas, while a smaller proportion of MAP2+ neurons (16% cortical layer I in subpial lesions, Figure 6Q; 17% field I in subependymal lesions, Figure 6S) and GFAP+ astrocytes (31% cortical layer I in subpial lesions, Figure 6Q; 23% field I in subependymal lesions, Figure 6S) expressing fibrinogen were noted.

Complement, another abundant serum protein, but not included in the CSF analysis, was detected at the perivascular spaces, the stroma and epithelium of the CP and in the adjacent subependymal space (complement C1q, fragments Bb, C3b, C4d and C1-inhibitor) (Supplem. Figure 1A–E), with terminal complement cascade activation, C5b-9, restricted to the vasculature and stroma of the CP (Figure SF–H).

4 | DISCUSSION

It is likely that the earliest inflammatory changes in the MS brain occur due to an increased permeability of the BBB that specifically allows activated immune cells into the brain parenchyma. With successive inflammatory episodes, the immune cells then become nested within the CNS, establishing an intrathecal compartmentalized immune niche. The consequence of this is a persistently inflammatory milieu in close contact to the brain parenchyma [3]. The CP is one of several gateways to immune sequestration in the CNS and CP inflammation may be another important surrogate marker of MS-specific compartmentalized inflammatory response.

In our comprehensive neuropathological analysis, in which we have combined quantitative scoring of infiltrating cells, molecular characterization of CP inflammation, and paired CSF analysis, we show that the CP inflammation is profound in some cases, associates with a more extensive and active periventricular pathology, and is dominated by innate immune activation and by high CSF levels of fibrinogen. Recent clinical and MRI study demonstrated that CP volume is higher early in patients with radiologically isolated syndrome (RIS) versus healthy controls (HC) and is associated with lower thalamic volume and high number of periventricular lesions [33]. Therefore, imaging the CP and the assaying of intrathecal fibrinogen could be important and specific indices of disease activity and progression in a substantial proportion of MS patients [6–9, 34].

The inflammatory role played by the CP in the pathogenesis of MS, both in experimental autoimmune encephalomyelitis (EAE) models and post-mortem MS brains, has been previously examined [4, 5, 35, 36]. The presence of prominent damage of the thalamus, hippocampus and basal ganglia, all GM structures that are near the ventricular surface and the CP was demonstrated. Because of its strategic location between the peripheral circulation and the cerebrospinal fluid, the CP is hypothesized to have an important function, both in the routine immune surveillance of the CNS and in intracerebral inflammation in MS [2, 5, 6, 8], even in CIS [10], although further evidence in MS is needed.

In our study, CP inflammation was mainly associated with perivascular inflammatory infiltration and less with meningeal inflammation, supporting again the idea that inflammatory activity in these compartments is linked [37]. Interestingly, we observed the presence of an increased cellular infiltration of the tela choroidea.

FIGURE 5 Graphical representation of the widespread white matter (blue color mask) and grey matter (cortical and deep grey matter; red color mask) demyelination in MS cases characterized by substantial inflammation of the CP (A). The presence of lesions was mainly associated with periventricular white matter and hippocampus (A). Spearman correlation analysis (B) between CP inflammation and the other quantified neuropathological parameters shows significant positive correlation (darker red) between degree of CP inflammation and degree of perivascular inflammation (R: 0.509, p: 7.921×10^{-4}), with meningeal inflammation (R: 0.365, p: 0.021) and with the number of active lesions (R: 0.51, p: 3.524×10^{-5}) identified in the surrounding periventricular areas (B). Extensive subependymal active demyelination (C) with intense microglia activation, characterized by expression of MHC-class II, TMEM119, CD163, and iNOs (D–H) were detected in the hippocampus. Spearman correlation analysis between degree of CP inflammation and clinical features of the examined MS cases did not reveal any significant correlation (I). Survival analysis that compared the populations with (red line) and without (blue line) CP inflammation, with respect to the age at death did not found significantly difference (p: 0.391), even if a higher percentage of subjects without CP inflammation were characterized by later age at death (J). Scale bars: 500 μm (C), 200 μm (D), 100 μm (E–I).
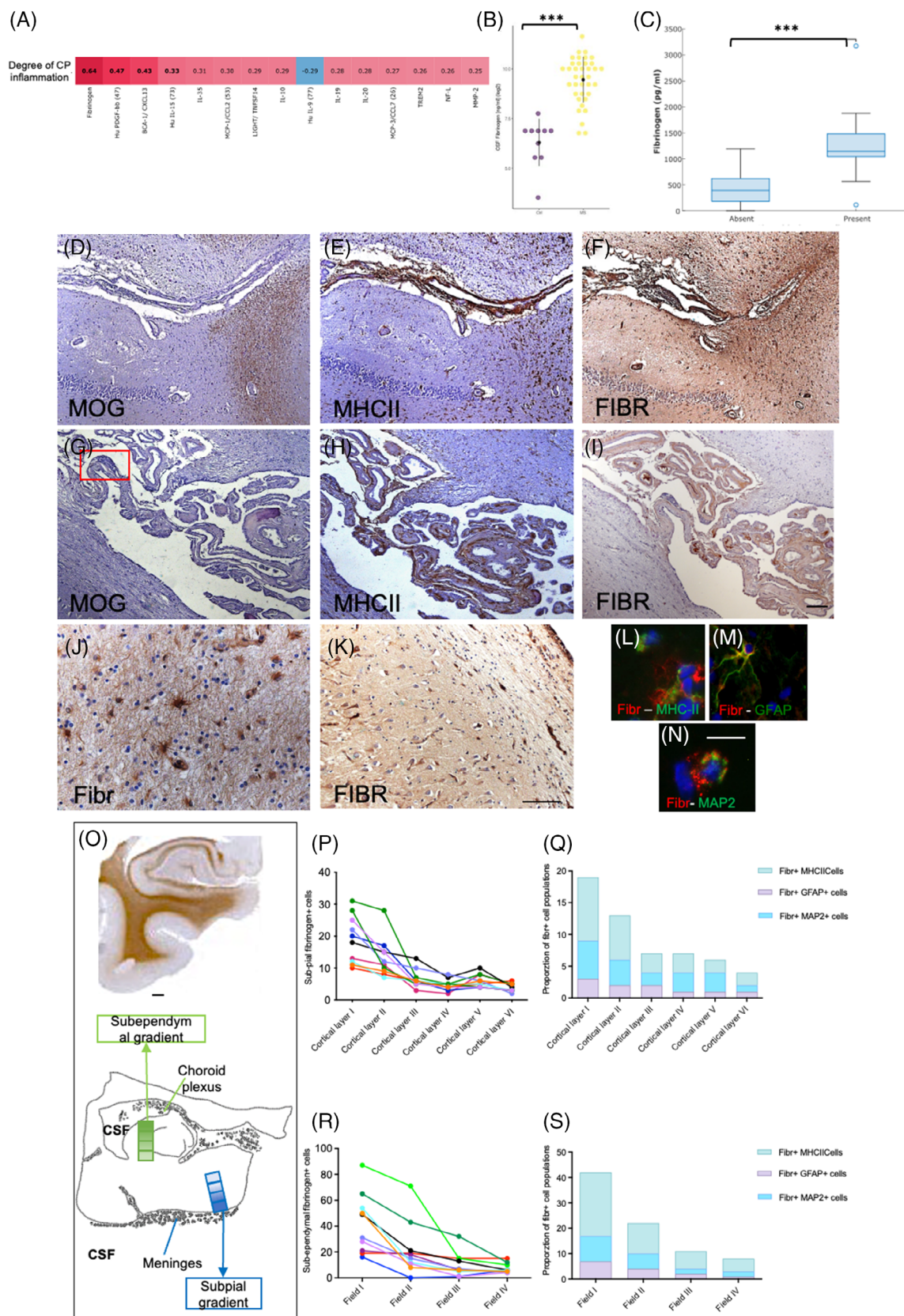
FIGURE 6 Legend on next page.

The tela choroidea is a specific region between the meningeal pia mater and underlying ependyma that is directly linked to the choroid plexus in the brain ventricles, where meningeal cells are supposed to abut the ventricular lining [38, 39]. We noted that inflammatory cells mainly accumulated in the meningeal side of the tela choroidea, suggesting that meninges may represent the most important MS route of cell traffic, entrance, and accumulation in the CNS [37].

The CP harbored significant numbers of innate immune cells, including MHCII+ macrophages with intracytoplasmic LFB myelin debris, CD68+, CD163+, TREM2, and TSPO+ populations of activated CP macrophages, and CD209/DC-Sign+ DC cells, which contrasted with the relative paucity of adaptive immune cells. That monocytes/ macrophages represent the largest and heterogenous class of CP immune cells in MS is corroborated by recent transcriptomic studies [40]. Stromal macrophages are located in the stromal space between the epithelial and endothelial layers, while epiplexus macrophages are usually along the apical epithelial surface. Our data, demonstrating consistent CP innate immune activity in progressive MS, support the hypothesis that both macrophage types may have higher turnover compared to other border-associated macrophages (meninges and perivascular spaces) and may play a fundamental role in regulation of the degree and duration of brain inflammation, viral entry, further immune cell recruitment and activation [41], possibly contributing to alterations of the CP permeability and size [42].

The high immunoreactivity in the CP for antigen presentation cell markers, including CD11c, TREM2, and TSPO, also demonstrated by using advanced in-situ hybridization technique, support the notion that innate immune activity persists in the CP of progressive MS brains contributing to disease activity. In addition, TSPO was found to be one of the genes overexpressed in the MS CP compared to other inflammatory genes in our multiplex analysis of a small number of cases. In the study of a pre-symptomatic cases, including those with radiologically isolated syndrome, who later developed clinically definite MS, Ricigliano and colleagues [43] demonstrated a 33% greater CP inflammation by TSPO PET in comparison to healthy controls. A population of CD163+ mononuclear phagocytes expressing TSPO were reported to account for much of this signal increase [43]. Monocytes/ macrophages are professional antigen presenting cells, that have the capacity to induce primary immune responses, in particular by inducing higher levels of Th1 (IFN-γ, TNF) and Th2 (IL-4, IL-13) cytokines compared with controls, while dendritic cells (DCs) from SPMS patients may only induce a polarized Th1 response [44]. The increased release of TNF, IL1β, IL6, type-I IFNs, and MHC class I and II expression may affect the CP inflammatory profile that we noted. Some of the first line treatments used in MS, such as glatiramer acetate, IFN-β, or anti-sphingosine phosphate were demonstrated to be able to synergistically suppress innate immune responses, such as inhibited CD1a and enhanced CD86 expression on MS DCs, contributing to the reduction of inflammatory response in MS [45].

The in-situ sequencing analysis, directly performed on choroid plexus, contributed to confirm the key role of innate immunity activation in the CP of progressive MS, as demonstrated by the elevated expression of TSPO and HLA-DRB1, even if also further genes related to adaptive immunity have been detected. The concurrent expression of genes that may be involved in recruitment (SELL/CD62L) [46] and regulation of activity of immune effector cells (RASGRP2), including several inflammatory mediators, such as IL17F, IL15, IL18, IL10, LTB, was also detected in the same areas [47]. Taken together these data suggest a key role for innate immune and T helper responses at the CP, not only at the beginning of the disease, but throughout the disease, possibly contributing to progression. It seems likely that chronic active lesions [25, 48, 49], perivascular spaces and leptomeninges, together with the CP [4, 5, 35], represent cerebral compartments where continuous stimulation of different immune components simultaneously contribute to drive disease inflammatory activity and progression. Interestingly, IL15 was also found as one of the CSF molecules linked to CP inflammation, suggesting the need of more in depth study of the potential role of this inflammatory mediator that was preciously demonstrated involved in direct cytotoxic effect mediated by macrophages and

FIGURE 6 Spearman correlation analysis (A) between CP inflammation and Among the 78 molecules examined in the CSF of the same MS cases: Degree of CP inflammation was found significantly and positively correlated (darker red and p values in bold) only with 4 markers: Fibrinogen (R: 0.640, p: 8.752×10^{-6}), PDGF-bb (R: 0.470, p: 0.002), CXCL13 (R: 0.428, p: 0.006) and IL15 (R: 0.327, p: 0.040) (A). CSF fibrinogen levels were significantly different not only in MS cases compared to controls (B; p: 0.0001), but also between the two populations (p: 8.654×10^{-6}) with and without CP inflammation (C). Neuropathological analyzing revealed fibrinogen immunoreactivity in active subpial cortical lesions (D–F) or subependymal lesions (G–I) in the hippocampus of the examined MS cases, mainly in cells morphologically resembling microglia, astrocytes or neuronal cells (J, K), as validated by double immunofluorescence (L–N). Schematic diagram of assessment of gradient of fibrinogen deposition from CSF surfaces towards inner brain regions, either at the pial or at the ependymal surface (O) according to the potential presence of a "surface-in" gradient in 10 of the examined MS cases characterized by the presence of at least one subpial cortical lesion and one subependymal one. Sub-pial (P, Q) and subependyma (R, S) gradients of fibrinogen+ cells increased density in the external areas close to CSF/brain interface. Most of the fibrinogen+ cells were identified as MHC+ microglia (Q, 59% cortical layer I in subpial lesions; S, 53% field I in subpendymal lesions), in particular in the most external areas, while less abundant proportion of MAP2+ neurons and GFAP+ astrocytes were identified in the same regions (Q, S). Scale bars: 1000 μm (O), 100 μm (D–K), 50 μm (L–N).

CD4+ T cells [50]. This supports the development and use of different technologies to fully map the immune-pathological mechanisms in CP, as well as in the other inflamed intracerebral compartments, to fully understand MS pathobiology and its potential driver. One of the most debated hypotheses support the idea that the over-time intracerebral persistence of antigen-presenting B cells generated through Epstein Bar virus (EBV)-mediated activation might continue to drive an uncontrolled, intrathecal immune response [51, 52]. A recent study has indeed found higher anti-EBV humoral response in patients with MS in association with increased CP volume changes detected by using MRI analysis, in particular in the later chronic stage of the disease, suggesting that CP may represent a continuous gateway through which EBV, and/or other potential immune-pathogenic factors, may influence MS clinical outcomes [53]. The overexpression of RASGRP2 [47], which could be involved in altered apoptosis and tumorigenesis of EBV-induced B and T cell signaling and homeostasis, in the CP of MS cases respect to controls further support the need of multidisciplinary studies to reveal the exact link between EBV and aberrant, chronic inflammatory response in MS.

We report that the degree of CP inflammation correlated with the number of active periventricular lesions. In particular, the high level of MHC-II and CD68 immunoreactivity in the CP and in the adjacent subependymal lesions, where TMEM119+ microglia followed a "surface-in" gradient, suggests why periventricular WM lesions and subpial GM lesions are so frequently observed in MS [17, 54, 55]. In cortical and deep GM, neuronal loss and glial activation are greatest in the outermost layers [17, 29]. This GM gradient has been replicated in vivo with magnetization transfer ratio (MTR) imaging, whereby gradients in GM and WM MTR are seen around the ventricles, with the most severe abnormalities abutting the ventricular surface, even in the earlier disease stages [55]. The level of meningeal inflammation, which was recently demonstrated to mediate changes of cortical microglial phenotype and, subsequently, enhanced cortical neurodegeneration [56], could have a major role in "surface-in" MS pathology [17]. Whether such microglial phenotypic changes and active demyelination occur at periventricular sites near the CP would be worth further investigating, in particular also in the progressive disease phase.

The blood-CSF (B-CSF) barrier localized in the CP could be partially permeable and simplify the passage of cytokines, chemokines and cells from blood to CSF. The high levels of CSF fibrinogen that differentiated MS cases with and without CP inflammation might suggest that the CP represents one of the routes of entrance of fibrinogen within the CSF. Fibrinogen deposition was previously found associated with BBB disruption, neuroinflammation and neurodegeneration in MS and several other neurological conditions [57]. The pattern of fibrinogen deposition was reflected by that of complement fragments, including classical complement proteins C1q and C4d, decorating the CP, emphasing the movement of serum proteins, which can induce inflammation, from blood to underlying tissues via the CP.

Fibrinogen, a protein of 340 kDa synthesized by hepatocytes and secreted into the vascular system, is also involved in the mechanisms of inflammation and tissue repair. Normally this protein is not present in healthy brain tissue, but increased BBB permeability, which occurs in many CNS pathologies, may favor the accumulation of fibrinogen in the cerebral parenchyma and its subsequent transformation into fibrin by perivascular factors [58, 59]. Numerous studies have demonstrated the neuropathological effects of fibrinogen in the CNS, where its cleavage by thrombin exposes a cryptic epitope of fibrin that binds CD11b and CD11c on microglia, macrophage and dendritic cells in CNS leading to their activation; in addition, axonal damage, inhibition of oligodendrocyte precursor differentiation and induction of astrocyte scar formation were also demonstrated related to be linked to abnormal fibrinogen levels [57]. Fibrinogen is detected in cortical GM MS lesions, where it accumulates on astrocyte processes in superficial cortical layers and in the cell soma of astrocytes and neurons in all layers of cerebral cortex [60]. Complement, like fibrinogen, is a potent activator of innate immune responses and products of complement activation are found at elevated levels in demyelinated cortical and deep GM tissues, together with increased numbers of complement receptor positive microglia. The link between fibrinogen deposition and activation of innate immunity is supported by experimental studies demonstrating that either genetically deficient mice for fibrinogen and anticoagulant-treated rats present reduced neuroinflammation, demyelination and axonal damage, as well as reduced microglia activation [19, 61–64]. All this experimental evidence strongly suggest that inflamed CP could be one of the routes of entry of fibrinogen and other serum proteins into the progressive MS CSF, where it may promote the "subependymal-in" gradient of microglial activation in periventricular areas. These data support the need of further experimental animal and/or cell culture models elucidating the pathological mechanisms mediated by fibrinogen and of the development of new therapeutic strategies by administrating monoclonal antibody targeting the cryptic fibrin epitope γ377-395 [63].

At the same time we found significant, even if low, correlation between degree of CP inflammation and high CSF levels of platelet-derived growth factor bb (PDGF-BB), supporting several findings showing that after the early inflammatory phases, the macrophage population assumes a wound-healing phenotype characterized by the production of numerous growth factors, including PDGF-BB [65] transforming growth factor β1 (TGF-β1), insulin-like growth factor 1 (IGF-1), and vascular endothelial growth factor a (VEGF-a), which may

locally stimulate cellular proliferation and activation and blood vessel development [66].

We did not find substantial correlation between degree of CP inflammation and different clinical features of the examined MS cases, suggesting that CP inflammatory activity in the progressive phase have no or only minor clinical impact. Previous studies did not find significant association between CP volume and clinical disability, as measured by the Expanded Disability Status Scale, EDSS [9], or with any longitudinal associations between changes in CP measures and clinical parameters, such as relapse rate over the course of the 5 years follow-up [12, 33]. These observations corroborate the hypothesis that CP may represent one of the main routes of leukocyte migration into the CNS at the beginning of the inflammatory attack [67], possibly contributing to periventricular pathology and volumetric changes, but with lower impact on the progressive pathology. It should also be considered that the absence of any correlation between CP inflammation and clinical milestones in our study MS cohort may be due to the small number of examined cases and the inclusion only of progressive MS cases. However, considering that we examined also cases with short disease duration (<15 years) and we did not find any correlation between degree of CP inflammation and disease duration and age at death, that at the contrary was extensively demonstrated in association with elevated level of meningeal inflammation [37], our data support the hypothesis that CP inflammatory changes have limited impact on the progressive phase.

Future work should continue to further elucidate the levels and type of exact inflammatory changes in early MS but also complementary multimodal biomarker and imaging measures to better reveal the real pathological events reflected by CP volume changes. In particular, whether alterations in CP structure and volume could have pathological effect in MS by modifying CSF composition and/or clearance, such in other neurological diseases [68] should be better examined. In addition, better understanding of the exact link of structural and inflammatory changes among different CNS barriers, including CP, leptomeninges, perivenular spaces, and glymphatic system [69], would be essential to obtain a comprehensive understanding of the possible determinants of MS immunopathology.

5 | CONCLUSIONS

We propose that CP inflammation, alongside other immune-pathological alterations at the expanding lesion edge and within the leptomeninges and perivascular spaces, represent a continous intracerebral routes of immune stimulation and possible diffusion of soluble mediators in progressive MS. CP inflammatory components may contribute to chronic intrathecal MS-specific compartmentalized inflammatory response and to

exacerbation of periventricular pathology, even without substantial effects on the clinical features observed at time of death. Fibrinogen, in particular, may represent one of the principal molecules directly or indirectly, through microglia activation, linked to MS surface-in gradient of tissue pathology.

Combining CP imaging and CSF molecular analysis may represent a useful and early prognostic biomarker of later disease inflammatory activity.

AUTHOR CONTRIBUTIONS

R.M., R.R., O.W.H. and S.M. contributed to the conception and study design; all authors contributed to the acquisition and analysis of data; R.M., S.H., M.M., A. M., M.K., L.G., L.M.W., O.W.H. and S.M. prepared figures and wrote the first draft; all authors reviewed the final submitted version.

ACKNOWLEDGMENTS

CONFLICT OF INTEREST STATEMENT

The authors declare no conflicts of interest related to this study.

DATA AVAILABILITY STATEMENT

The data that support the findings of this study are available on request from the corresponding author.

ORCID

R. Magliozzi https://orcid.org/0000-0001-8284-7763
L. Griffiths https://orcid.org/0000-0002-8713-3687
O. W. Howell https://orcid.org/0000-0003-2157-9157

REFERENCES

1. Kaur C, Rathnasamy G, Ling E-A. The choroid plexus in healthy and diseased brain. J Neuropathol Exp Neurol. 2016;75:198–213. https://doi.org/10.1093/jnen/nlv030
2. Kivisäkk P, Mahad DJ, Callahan MK, Trebst C, Tucky B, Wei T, et al. Human cerebrospinal fluid central memory CD4+ T cells: evidence for trafficking through choroid plexus and meninges via P-selectin. Proc Natl Acad Sci. 2003;100:8389–94. https://doi.org/10.1073/pnas.1433000100

3. Monaco S, Nicholas R, Reynolds R, Magliozzi R. Intrathecal inflammation in progressive multiple sclerosis. Int J Mol Sci. 2020; 21:8217. https://doi.org/10.3390/ijms21218217

4. Vercellino M, Votta B, Condello C, Piacentino C, Romagnolo A, Merola A, et al. Involvement of the choroid plexus in multiple sclerosis autoimmune inflammation: a neuropathological study. J Neuroimmunol. 2008;199:133–41. https://doi.org/10.1016/j.jneuroim.2008.04.035

5. Rodríguez-Lorenzo S, Konings J, van der Pol S, Kamermans A, Amor S, van Horssen J, et al. Inflammation of the choroid plexus in progressive multiple sclerosis: accumulation of granulocytes and T cells. Acta Neuropathol Commun. 2020;8:9. https://doi.org/10.1186/s40478-020-0885-1

6. Kim H, Lim Y-M, Kim G, Lee E-J, Lee JH, Kim HW, et al. Choroid plexus changes on magnetic resonance imaging in multiple sclerosis and neuromyelitis optica spectrum disorder. J Neurol Sci. 2020;415:116904. https://doi.org/10.1016/j.jns.2020.116904

7. Klistorner S, Barnett MH, Parratt J, Yiannikas C, Graham SL, Klistorner A. Choroid plexus volume in multiple sclerosis predicts expansion of chronic lesions and brain atrophy. Ann Clin Transl Neurol. 2022;9:1528–37. https://doi.org/10.1002/acn3.51644

8. Müller J, Sinnecker T, Wendebourg MJ, Schläger R, Kuhle J, Schädelin S, et al. Choroid plexus volume in multiple sclerosis vs neuromyelitis optica spectrum disorder. Neurol Neuroimmunol Neuroinflamm. 2022;9:e1147. https://doi.org/10.1212/NXI.0000000000001147

9. Ricigliano VAG, Morena E, Colombi A, Tonietto M, Hamzaoui M, Poirion E, et al. Choroid plexus enlargement in inflammatory multiple sclerosis: 3.0-T MRI and translocator protein PET evaluation. Radiology. 2021;301:166–77. https://doi.org/10.1148/radiol.2021204426

10. Klistorner S, Van der Walt A, Barnett MH, Butzkueven H, Kolbe S, Parratt J, et al. Choroid plexus volume is enlarged in clinically isolated syndrome patients with optic neuritis. Mult Scler J. 2023;29:540–8. https://doi.org/10.1177/13524585231157206

11. Margoni M, Preziosa P, Storelli L, Gueye M, Moiola L, Filippi M, et al. Paramagnetic rim and core sign lesions in paediatric multiple sclerosis patients. J Neurol Neurosurg Psychiatry. 2023;94:1–3. https://doi.org/10.1136/jnnp-2022-331027

12. Bergsland N, Dwyer MG, Jakimovski D, Tavazzi E, Benedict RHB, Weinstock-Guttman B, et al. Association of Choroid Plexus Inflammation on MRI with clinical disability progression over 5 years in patients with multiple sclerosis. Neurology. 2023;100:e911–20. https://doi.org/10.1212/WNL.0000000000201608

13. Preziosa P, Pagani E, Meani A, Storelli L, Margoni M, Yudin Y, et al. Chronic active lesions and larger choroid plexus explain cognition and fatigue in multiple sclerosis. Neurol Neuroimmunol Neuroinflamm. 2024;11:1–14. https://doi.org/10.1212/NXI.0000000000200205

14. Howell OW, Reeves CA, Nicholas R, Carassiti D, Radotra B, Gentleman SM, et al. Meningeal inflammation is widespread and linked to cortical pathology in multiple sclerosis. Brain. 2011;134:2755–71. https://doi.org/10.1093/brain/awr182

15. Magliozzi R, Howell OW, Nicholas R, Cruciani C, Castellaro M, Romualdi C, et al. Inflammatory intrathecal profiles and cortical damage in multiple sclerosis. Ann Neurol. 2018;83:739–55. https://doi.org/10.1002/ana.25197

16. James RE, Schalks R, Browne E, Eleftheriadou I, Munoz CP, Mazarakis ND, et al. Persistent elevation of intrathecal pro-inflammatory cytokines leads to multiple sclerosis-like cortical demyelination and neurodegeneration. Acta Neuropathol Commun. 2020;8:66. https://doi.org/10.1186/s40478-020-00938-1

17. Magliozzi R, Fadda G, Brown RA, Bar-Or A, Howell OW, Hametner S, et al. "Ependymal-in" gradient of thalamic damage in progressive multiple sclerosis. Ann Neurol. 2022;92:670–85. https://doi.org/10.1002/ana.26448

18. Picon C, Jayaraman A, James R, Beck C, Gallego P, Witte ME, et al. Neuron-specific activation of necroptosis signaling in multiple sclerosis cortical grey matter. Acta Neuropathol. 2021; 141:585–604. https://doi.org/10.1007/s00401-021-02274-7

19. Cooze BJ, Dickerson M, Loganathan R, Watkins LM, Grounds E, Pearson BR, et al. The association between neurodegeneration and local complement activation in the thalamus to progressive multiple sclerosis outcome. Brain Pathol. 2022;32:e13054.

20. De Groot CJA. Post-mortem MRI-guided sampling of multiple sclerosis brain lesions: increased yield of active demyelinating and (p)reactive lesions. Brain. 2001;124:1635–45. https://doi.org/10.1093/brain/124.8.1635

21. Magliozzi R, Howell O, Vora A, Serafini B, Nicholas R, Puopolo M, et al. Meningeal B-cell follicles in secondary progressive multiple sclerosis associate with early onset of disease and severe cortical pathology. Brain. 2006;130:1089–104. https://doi.org/10.1093/brain/awm038

22. Bankhead P, Loughrey MB, Fernández JA, Dombrowski Y, McArt DG, Dunne PD, et al. QuPath: open source software for digital pathology image analysis. Sci Rep. 2017;7:16878. https://doi.org/10.1038/s41598-017-17204-5

23. Metz I, Weigand SD, Popescu BFG, Frischer JM, Parisi JE, Guo Y, et al. Pathologic heterogeneity persists in early active multiple sclerosis lesions. Ann Neurol. 2014;75:728–38. https://doi.org/10.1002/ana.24163

24. Van Der Valk P, De Groot CJA. Staging of multiple sclerosis (MS) lesions: pathology of the time frame of MS. Neuropathol Appl Neurobiol. 2000;26:2–10. https://doi.org/10.1046/j.1365-2990.2000.00217.x

25. Zrzavy T, Hametner S, Wimmer I, Butovsky O, Weiner HL, Lassmann H. Loss of 'homeostatic' microglia and patterns of their activation in active multiple sclerosis. Brain. 2017;140:1900–13. https://doi.org/10.1093/brain/awx113

26. Nicholas R, Magliozzi R, Marastoni D, Howell O, Roncaroli F, Muraro P, et al. High levels of perivascular inflammation and active demyelinating lesions at time of death associated with rapidly progressive multiple sclerosis disease course: a retrospective postmortem cohort study. Ann Neurol. 2024;95:706–19. https://doi.org/10.1002/ana.26870

27. Reynolds R, Roncaroli F, Nicholas R, Radotra B, Gveric D, Howell O. The neuropathological basis of clinical progression in multiple sclerosis. Acta Neuropathol. 2011;122:155–70. https://doi.org/10.1007/s00401-011-0840-0

28. Moore GRW, Laule C, Leung E, Pavlova V, Morgan BP, Esiri MM. Complement and humoral adaptive immunity in the human choroid plexus: roles for stromal concretions, basement membranes, and epithelium. J Neuropathol Exp Neurol. 2016;75:415–28. https://doi.org/10.1093/jnen/nlw017

29. Magliozzi R, Howell OW, Reeves C, Roncaroli F, Nicholas R, Serafini B, et al. A gradient of neuronal loss and meningeal inflammation in multiple sclerosis. Ann Neurol. 2010;68:477–93. https://doi.org/10.1002/ana.22230

30. Hernandez I., Xiaoyan Qian, Jana Laláková, Toon Verheyen, Markus Hilscher, Malte Kühnemund, (2019) Mapping brain cell types with CARTANA in situ sequencing on the Nikon Ti2-E microscope.

31. Lee JH, Daugharthy ER, Scheiman J, Kalhor R, Ferrante TC, Terry R, et al. Fluorescent in situ sequencing (FISSEQ) of RNA for gene expression profiling in intact cells and tissues. Nat Protoc. 2015;10:442–58. https://doi.org/10.1038/nprot.2014.191

32. Gyllborg D, Langseth CM, Qian X, Choi E, Salas SM, Hilscher MM, et al. Hybridization-based *in situ* sequencing (HybISS) for spatially resolved transcriptomics in human and mouse brain tissue. Nucleic Acids Res. 2020;48:e112. https://doi.org/10.1093/nar/gkaa792

33. Landes-Château C, Ricigliano VA, Mondot L, Thouvenot E, Labauge P, Louapre C, et al. Choroid plexus enlargement correlates with periventricular pathology but not with disease activity in radiologically isolated syndrome. Mult Scler. 2024;30:1278–89. https://doi.org/10.1177/13524585241272943

34. Ryu JK, Petersen MA, Murray SG, Baeten KM, Meyer-Franke A, Chan JP, et al. Blood coagulation protein fibrinogen promotes autoimmunity and demyelination via chemokine release and antigen presentation. Nat Commun. 2015;6:8164. https://doi.org/10.1038/ncomms9164

35. Papadopoulos D, Dukes S, Patel R, Nicholas R, Vora A, Reynolds R. Substantial Archaeocortical atrophy and neuronal loss in multiple sclerosis. Brain Pathol. 2009;19:238–53. https://doi.org/10.1111/j.1750-3639.2008.00177.x

36. Reboldi A, Coisne C, Baumjohann D, Benvenuto F, Bottinelli D, Lira S, et al. C-C chemokine receptor 6–regulated entry of TH-17 cells into the CNS through the choroid plexus is required for the initiation of EAE. Nat Immunol. 2009;10:514–23. https://doi.org/10.1038/ni.1716

37. Magliozzi R, Howell OW, Calabrese M, Reynolds R. Meningeal inflammation as a driver of cortical grey matter pathology and clinical progression in multiple sclerosis. Nat Rev Neurol. 2023;19:461–76. https://doi.org/10.1038/s41582-023-00838-7

38. Lun MP, Monuki ES, Lehtinen MK. Development and functions of the choroid plexus–cerebrospinal fluid system. Nat Rev Neurosci. 2015;16:445–57. https://doi.org/10.1038/nrn3921

39. Zemmoura I, Velut S, François P. The choroidal fissure: anatomy and surgical implications. Adv Tech Stand Neurosurg. 2012;38:97–113.

40. Dani N, Herbst RH, McCabe C, Green GS, Kaiser K, Head JP, et al. A cellular and spatial map of the choroid plexus across brain ventricles and ages. Cell. 2021;184:3056–74.

41. Cui J, Xu H, Lehtinen MK. Macrophages on the margin: choroid plexus immune responses. Trends Neurosci. 2021;44:864–75. https://doi.org/10.1016/j.tins.2021.07.002

42. Johanson C. Choroid plexus blood-CSF barrier: major player in brain disease modeling and Neuromedicine. J Neurol Neuromed. 2018;3:39–58. https://doi.org/10.29245/2572.942X/2018/4.1194

43. Ricigliano VAG, Louapre C, Poirion E, Colombi A, Yazdan Panah A, Lazzarotto A, et al. Imaging characteristics of choroid plexuses in Presymptomatic multiple sclerosis. Neurol Neuroimmunol Neuroinflamm. 2022;9:e200026. https://doi.org/10.1212/NXI.0000000000200026

44. Karni A, Abraham M, Monsonego A, Cai G, Freeman GJ, Hafler D, et al. Innate immunity in multiple sclerosis: myeloid dendritic cells in secondary progressive multiple sclerosis are activated and drive a proinflammatory immune response. J Immunol. 2006;177:4196–202. https://doi.org/10.4049/jimmunol.177.6.4196

45. Hussien Y, Sanna A, Söderström M, Link H, Huang Y-M. Glatiramer acetate and IFN-β act on dendritic cells in multiple sclerosis. J Neuroimmunol. 2001;121:102–10. https://doi.org/10.1016/S0165-5728(01)00432-5

46. Engelhardt B. Immune cell entry into the central nervous system: involvement of adhesion molecules and chemokines. J Neurol Sci. 2008;274:23–6. https://doi.org/10.1016/j.jns.2008.05.019

47. Jelcic I, Al Nimer F, Wang J, Lentsch V, Planas R, Jelcic I, et al. Memory B cells activate brain-homing, autoreactive CD4+ T cells in multiple sclerosis. Cell. 2018;175:85–100.e23. https://doi.org/10.1016/j.cell.2018.08.011

48. Absinta M, Maric D, Gharagozloo M, Garton T, Smith MD, Jin J, et al. A lymphocyte–microglia–astrocyte axis in chronic active multiple sclerosis. Nature. 2021;597:709–14. https://doi.org/10.1038/s41586-021-03892-7

49. Dal-Bianco A, Grabner G, Kronnerwetter C, Weber M, Kornek B, Kasprian G, et al. Long-term evolution of multiple sclerosis iron rim lesions in 7 T MRI. Brain. 2021;144:833–47.

50. Broux B, Mizee MR, Vanheusden M, van der Pol S, van Horssen J, Van Wijmeersch B, et al. IL-15 amplifies the pathogenic properties of CD4+CD28- T cells in multiple sclerosis. J Immunol. 2015;194:2099–109. https://doi.org/10.4049/jimmunol.1401547

51. Aloisi F, Giovannoni G, Salvetti M. Epstein-Barr virus as a cause of multiple sclerosis: opportunities for prevention and therapy. Lancet Neurol. 2023;22:338–49. https://doi.org/10.1016/S1474-4422(22)00471-9

52. Bjornevik K, Münz C, Cohen JI, Ascherio A. Epstein–Barr virus as a leading cause of multiple sclerosis: mechanisms and implications. Nat Rev Neurol. 2023;19:160–71. https://doi.org/10.1038/s41582-023-00775-5

53. Jakimovski D, Zivadinov R, Ramanathan M, Weinstock-Guttman B, Tavazzi E, Dwyer MG, et al. Greater humoral EBV response may be associated with choroid plexus inflammation in progressive MS. J Neurovirol. 2024. https://doi.org/10.1007/s13365-024-01231-w

54. Kutzelnigg A, Lucchinetti CF, Stadelmann C, Brück W, Rauschka H, Bergmann M, et al. Cortical demyelination and diffuse white matter injury in multiple sclerosis. Brain. 2005;128:2705–12. https://doi.org/10.1093/brain/awh641

55. Pardini M, Brown JWL, Magliozzi R, Reynolds R, Chard DT. Surface-in pathology in multiple sclerosis: a new view on pathogenesis? Brain. 2021;144:1646–54. https://doi.org/10.1093/brain/awab025

56. van Olst L, Rodriguez-Mogeda C, Picon C, Kiljan S, James RE, Kamermans A, et al. Meningeal inflammation in multiple sclerosis induces phenotypic changes in cortical microglia that differentially associate with neurodegeneration. Acta Neuropathol. 2021;141:881–99. https://doi.org/10.1007/s00401-021-02293-4

57. Petersen MA, Ryu JK, Akassoglou K. Fibrinogen in neurological diseases: mechanisms, imaging and therapeutics. Nat Rev Neurosci. 2018;19:283–301. https://doi.org/10.1038/nrn.2018.13

58. Akassoglou K, Strickland S. Nervous system pathology: the fibrin perspective. Biol Chem. 2002;383:37–45. https://doi.org/10.1515/BC.2002.004

59. Thomas WS, Mori E, Copeland BR, Yu JQ, Morrissey JH, del Zoppo GJ. Tissue factor contributes to microvascular defects after focal cerebral ischemia. Stroke. 1993;24:847–53. https://doi.org/10.1161/01.STR.24.6.847

60. Yates RL, Esiri MM, Palace J, Jacobs B, Perera R, DeLuca GC. Fibrin(ogen) and neurodegeneration in the progressive multiple sclerosis cortex. Ann Neurol. 2017;82:259–70. https://doi.org/10.1002/ana.24997

61. Davalos D, Ryu JK, Merlini M, Baeten KM, Le Moan N, Petersen MA, et al. Fibrinogen-induced perivascular microglial clustering is required for the development of axonal damage in neuroinflammation. Nat Commun. 2012;3:1227.

62. Evans R, Watkins LM, Hawkins K, Santiago G, Demetriou C, Naughton M, et al. Complement activation and increased anaphylatoxin receptor expression are associated with cortical grey matter lesions and the compartmentalised inflammatory response of multiple sclerosis. Front Cell Neurosci. 2023;17. https://doi.org/10.3389/fncel.2023.1094106

63. Ryu JK, Rafalski VA, Meyer-Franke A, Adams RA, Poda SB, Rios Coronado PE, et al. Fibrin-targeting immunotherapy protects against neuroinflammation and neurodegeneration. Nat Immunol. 2018;19:1212–23. https://doi.org/10.1038/s41590-018-0232-x

64. Watkins LM, Neal JW, Loveless S, Michailidou I, Ramaglia V, Rees MI, et al. Complement is activated in progressive multiple sclerosis cortical grey matter lesions. J Neuroinflamm. 2016;13:161. https://doi.org/10.1186/s12974-016-0611-x

65. Shimokado K, Umezawa K, Ogata J. Tyrosine kinase inhibitors inhibit multiple steps of the cell cycle of vascular smooth muscle cells. Exp Cell Res. 1995;220:266–73. https://doi.org/10.1006/excr.1995.1315

66. Wynn TA, Vannella KM. Macrophages in tissue repair, regeneration, and fibrosis. Immunity. 2016;44:450–62. https://doi.org/10.1016/j.immuni.2016.02.015

67. Ransohoff RM, Kivisäkk P, Kidd G. Three or more routes for leukocyte migration into the central nervous system. Nat Rev Immunol. 2003;3:569–81. https://doi.org/10.1038/nri1130

68. Tadayon E, Pascual-Leone A, Press D, Santarnecchi E, Alzheimer's Disease Neuroimaging Initiative. Choroid plexus volume is

associated with levels of CSF proteins: relevance for Alzheimer's and Parkinson's disease. Neurobiol Aging. 2020;89:108–17. https://doi.org/10.1016/j.neurobiolaging.2020.01.005

69. Mapunda JA, Tibar H, Regragui W, Engelhardt B. How does the immune system enter the brain? Front Immunol. 2022;13:805657. https://doi.org/10.3389/fimmu.2022.805657

SUPPORTING INFORMATION

Additional supporting information can be found online in the Supporting Information section at the end of this article.